Long-range transmission of solitons in random media

Josselin Garnier[a] and Fatkhulla Kh. Abdullaev[b]

[a] Centre de Mathématiques Appliquées, Ecole Polytechnique, 91128 Palaiseau Cedex, France
[b] Physical-Technical Institute, 700084, Tashkent 84, G. Mavlyanov Str., 2-B, Uzbekistan

ABSTRACT

A statistical approach of the propagation of solitons in media with spatially random perturbations is developed. Applying the inverse scattering transform several regimes are put into evidence which are determined by the mass and the velocity of the incoming soliton and also by the correlation length of the perturbation. The mass of the transmitted soliton may tend to zero exponentially (as a function of the size of the slab) or following a power law; or else the soliton may keep its mass if it is initially large enough, while its velocity decreases at a logarithmic rate or even slower. Numerical simulations are in good agreement with the theoretical results.

Keywords: Soliton, nonlinear Schrödinger equation, random perturbations.

1. INTRODUCTION

It is well-known that in one-dimensional random linear media strong localization occurs, which means in particular that the transmitted intensity decays exponentially as a function of the size of the medium.[1] This paper is a contribution of the study competition between nonlinearity and localization effects. There exist some results for the stationary case. It has been shown that the presence of a slight nonlinearity competes with the effects which lead to exponential localization and allows some probability of transmission,[2] even though there must be some decay.[3] In Ref.4 a power law decay of the transmittivity is demonstrated by the use of the embedding method. These results are for steady waves and do not apply to a time-dependent problem since the superposition principle fails due to nonlinearity. Kivshar[5] was the first one to show that the nonlinearity does have an effect in a time-dependent problem, by studying the propagation of a soliton through a slab of random nonlinear medium. We shall consider in this paper a random Schrödinger equation with cubic nonlinearity, and discuss the ability of a soliton to propagate without distortion.

2. SOLITARY WAVES

A solitary wave is a wave that propagates without change of form or diminution of speed. The study of solitary waves began in 1838 with the observation by J. Scott Russel of such a water wave while riding on horseback along a channel. However no mathematical theory available at the time predicted a solitary wave. The problem was resolved in 1895 by Korteweg and de Vries who derived an equation (now known as the KdV equation) which governs small shallow-water waves.[6] Boussinesq in 1871 also derived a nonlinear wave equation governing such long waves.[7] Despite this early work no further application was discovered until the 1960's. In 1967 Gardner, Green, Kruskal, and Miura first discovered an original method of solution of KdV by applying an implicit linearization of the equation: the so-called inverse scattering transform.[8] Lax (1968) considerably generalized these ideas,[9] and Zakharov and Shabat (1972) showed that the method worked for the nonlinear Schrödinger (NLS) equation.[10] At this time it was known that the NLS equation describes the propagation of short pulses in mono-mode optical fibers.[11] Hasegawa (1973) then claimed that the soliton was the ideal candidate to be the information bit for the next generation of optical fibers.[12] In order to confirm this hope, it is relevant to study the behavior of a soliton when it propagates through weakly perturbed media over very large distances. In this paper we shall restrict ourselves to the case of the NLS equation with spatially random coefficients, but the method can be generalized to other types of random perturbations (time-dependent) and other completely integrable systems. Note that the NLS equation with a random potential has been studied by many different authors both theoretically[5,13–15] and numerically.[16,17] We shall present in the following a rigorous application of the inverse scattering transform that allows us to derive relevant results for a large class of perturbations.

Send correspondence to J. Garnier : Josselin.Garnier@polytechnique.fr

3. AN INTRODUCTION TO THE INVERSE SCATTERING TRANSFORM

For more detail about the following statements and their proofs we refer to Refs. 18,19. The scattering transform aims at studying the solutions of nonlinear partial differential equations of the type $u_t = F(u)$ with rapidly decaying initial conditions. It can be applied in the case where the evolution equation is equivalent to an equality between linear operators:

$$\frac{\partial L(u)}{\partial t} + [L, A] = 0. \tag{1}$$

It is based on the fact that $u(t,.)$ can be characterized by some spectral data of the operator $L(u(t,.))$. The homogeneous nonlinear Schrödinger equation (NLS):

$$iu_t + u_{xx} + 2|u|^2 u = 0 \tag{2}$$

can be expressed in the form (1) if we set

$$L(u) = iP\frac{\partial}{\partial x} + Q(u), \text{ with } P = \begin{pmatrix} 1 & 0 \\ 0 & -1 \end{pmatrix} \text{ and } Q(u) = \begin{pmatrix} 0 & u^* \\ -u & 0 \end{pmatrix}.$$

The operator A is of the type $-2iP\frac{\partial^2}{\partial x^2} + C(u)$, with $C(u) \to 0$ when $u \to 0$, $u_x \to 0$. The domain of $L(u)$ is the space $\mathbb{H}^1(\mathbb{R})$,

$$\mathbb{H}^1(\mathbb{R}) = \left\{\psi \text{ such that } \psi \in \mathbb{L}^2(\mathbb{R}), \psi_x \in \mathbb{L}^2(\mathbb{R})\right\},$$

which is a dense subset of the Hilbert space $\mathbb{L}^2(\mathbb{R})$:

$$\mathbb{L}^2(\mathbb{R}) = \left\{\psi = \psi_1 \mathbf{e_1} + \psi_2 \mathbf{e_2}, \psi_j \in L^2(\mathbb{R})\right\}, \quad \mathbf{e_1} = \begin{pmatrix} 1 \\ 0 \end{pmatrix}, \quad \mathbf{e_2} = \begin{pmatrix} 0 \\ 1 \end{pmatrix}$$

equipped with the scalar product:

$$\langle \psi, \phi \rangle = \int_{-\infty}^{+\infty} dx \psi_1^* \phi_1(x) + \psi_2^* \phi_2(x).$$

Operator $L(0)$. $L(0)$ is self-adjoint. The real axis constitutes its essential spectrum. The eigenspace associated with the eigenvalue $\lambda \in \mathbb{R}$ has dimension 2 and admits the couple $\left(\mathbf{e_1} e^{-i\lambda x}, \mathbf{e_2} e^{i\lambda x}\right)$ as a base. Besides the point spectrum of $L(0)$ is empty, because the non-trivial solutions of $v_x = i\lambda v$ are not in $L^2(\mathbb{R})$.

Essential spectrum of the operator $L(u(t = t_0, .))$. Let us consider the spectral problem associated with the operator $L(u) = L(0) + Q(u)$:

$$L(u(t,x))\psi(t,x) = \lambda(t)\psi(t,x), \quad \psi = \psi_1 \mathbf{e_1} + \psi_2 \mathbf{e_2}. \tag{3}$$

If $u(t = t_0, .) \in L^1(\mathbb{R})$, then $Q(u)$ is $L(0)$-compact. As a consequence of the Weyl theorem, the essential spectrum of $L(u)$ is equal to the real axis. Eq. (3) actually admits two linearly independent solutions when λ is real. We introduce the so-called Jost functions f and g, defined as the eigenfunctions of $L(u)$ associated with the real eigenvalue λ which satisfy the following boundary conditions:

$$f(x,\lambda) \overset{x \to +\infty}{\longrightarrow} \mathbf{e_2} e^{i\lambda x}, \quad g(x,\lambda) \overset{x \to -\infty}{\longrightarrow} \mathbf{e_1} e^{-i\lambda x}.$$

If we denote by $\bar{\psi}$ the vector $(\psi_2^*, -\psi_1^*)$ associated with a vector ψ solution of (3), then $\bar{\psi}$ is a solution of $L\bar{\psi} = \lambda^* \bar{\psi}$. In the case of a real eigenvalue, ψ and $\bar{\psi}$ are linearly independent and form a base of the space of the solutions of (3). It can then be proved that the Jost functions are related by:

$$g(x,\lambda) = a(\lambda)\bar{f}(x,\lambda) + b(\lambda)f(x,\lambda), \quad f(x,\lambda) = -a(\lambda)\bar{g}(x,\lambda) + b^*(\lambda)g(x,\lambda). \tag{4}$$

Substituting the second equality into the first one, we also exhibit the following conservation relation:

$$|a(\lambda)|^2 + |b(\lambda)|^2 = 1. \tag{5}$$

Using (3) we get two more conservation relations which concern the norms of the Jost functions f and g:

$$|f_1(x,\lambda)|^2 + |f_2(x,\lambda)|^2 = 1, \qquad |g_1(x,\lambda)|^2 + |g_2(x,\lambda)|^2 = 1.$$

Multiplying the first equality of (4) by the vector $\bar{f}^*$, we get an explicit representation of the coefficient a as the Wronskian of f and g:

$$a(\lambda) = g_1(x,\lambda) f_2(x,\lambda) - g_2(x,\lambda) f_1(x,\lambda). \tag{6}$$

We are able to provide a more explicit representation of the Jost functions f and g. Denoting $\tilde{f}_1(x,\lambda) = e^{i\lambda x} f_1(x,\lambda)$ and $\tilde{f}_2(x,\lambda) = e^{-i\lambda x} f_2(x,\lambda)$, we can find from (3) that $\tilde{f}$ satisfies a system of integral equations. Besides $\tilde{f}_1$ can be eliminated from this system by substitution, so that we get a closed equation for $\tilde{f}_2$, whose solution is:

$$\tilde{f}_2(x,\lambda) = 1 + \int_x^\infty dy M(y,x,\lambda) \left(1 + \int_y^\infty dz M(z,x,\lambda)\,(...)\right),$$

where $M(y,x,\lambda) = -u^*(y)\int_x^y dz u(z) e^{2i\lambda(y-z)}$. This expression holds true when $u \in L^1$, because the associated sequence absolutely converges. The function $\tilde{f}_1$ also admits a similar representation. Let us examine carefully the properties of $\tilde{f}$. If $y \mapsto |y|^n |u(y)| \in L^1$, then $\tilde{f}_1$ and $\tilde{f}_2$ are of class $\mathcal{C}^n$ over the real axis. Besides, if $u \in L^1$, then $\tilde{f}_1$ and $\tilde{f}_2$ can be analytically continued in the upper complex half-plane $\mathrm{Im}(\lambda) \geq 0$ where they have no singularity. Indeed, in view of the definition of M one can see that the exponential term has a norm equal to $e^{-2\mathrm{Im}\lambda(y-z)}$ (remember that we integrate over the domain $y - z > 0$) which decays faster than any polynomial term brought by the λ-derivatives.

Point spectrum of the operator $L(u(t=t_0,.))$. From (6) we can define an analytic continuation of $a(\lambda)$ over the upper complex half-plane. A noticeable feature then appears. If λ_r is a zero of $a(\lambda)$, then f and g are linearly dependent, so there exists a coefficient ρ_r such that $g(x,\lambda_r) = \rho_r f(x,\lambda_r)$. The corresponding eigenfunction is bounded and decays exponentially as $x \to +\infty$ (because $|f| \sim e^{-\mathrm{Im}\lambda_r x}$) and as $x \to -\infty$ (because $|g| \sim e^{+\mathrm{Im}\lambda_r x}$. Thus λ_r is an element of the point spectrum of $L(u)$. Moreover we can compute from (3) and (6) the λ-derivative of a at $\lambda = \lambda_r$:

$$a'(\lambda_r) = -2i\rho_r \int_{-\infty}^{+\infty} dx f_1 f_2(x,\lambda_r). \tag{7}$$

It can then be proved that the set $(a(\lambda), b(\lambda), \lambda_r, \rho_r, a'(\lambda_r))$ characterizes the Jost functions f and g as well as the solution u. The inverse transform is essentially based on the resolution of the linear integro-differential Gelfand-Levitan-Marchenko equation, whose entries are constituted by the set $(a, b, \lambda_r, \rho_r, a'(\lambda_r))$:

$$\begin{aligned} K_1(x,y) &= \Phi^*(x+y) - \int_x^\infty K_1(x,y'') \int_x^\infty \Phi^*(y+y')\Phi(y'+y'')dy'dy'', \\ K_2(x,y) &= -\int_x^\infty K_1^*(x,y')\Phi^*(y+y')dy', \\ \text{where } \Phi(y) &= -\sum_r \frac{i\rho_r}{a'(\lambda_r)} e^{i\lambda_r y} + \frac{1}{2\pi}\int_{-\infty}^{+\infty} \frac{b(\lambda)}{a(\lambda)} e^{i\lambda y} d\lambda. \end{aligned} \tag{8}$$

We can get the eigenvector f from the kernel K solution of (8):

$$f(x,\lambda) = \mathbf{e_2} e^{i\lambda x} + \int_x^\infty K(x,y) e^{i\lambda y} dy. \tag{9}$$

We then obtain u by the formula $u(x) = -2iK_1^*(x,x)$. The study of the inverse problem associated with the operator $L(u)$ has not yet been completely achieved. In particular the precise characterization of the spectral data which lead to well-defined potentials u has not yet been completed. However, in the case where the initial condition u_0 is rapidly decaying so that it satisfies $x \mapsto |x|^n |u_0|(x) \in L^1$ for any n, the inverse scattering can be rigorously achieved.[18]

The great advantage of the method is that the evolution equations of the scattering data are uncoupled:

$$a(t,\lambda) = a(t_0,\lambda), \quad b(t,\lambda) = b(t_0,\lambda) e^{-4i\lambda^2(t-t_0)}, \quad \rho_r(t) = \rho_r(t_0) e^{-4i\lambda_r^2(t-t_0)}.$$

To sum up, the scattering transform involves the following operations:

$$\begin{array}{ccc} u(t_0,x) & \overset{\text{direct scatt.}}{\longrightarrow} & (a,b,\lambda_r,\rho_r,a'(\lambda_r))\,(t_0) \\ \text{NLS}\downarrow & & \downarrow \text{uncoupled evolution equations} \\ u(t,x) & \overset{\text{inverse scatt.}}{\longleftarrow} & (a,b,\lambda_r,\rho_r,a'(\lambda_r))\,(t) \end{array}$$

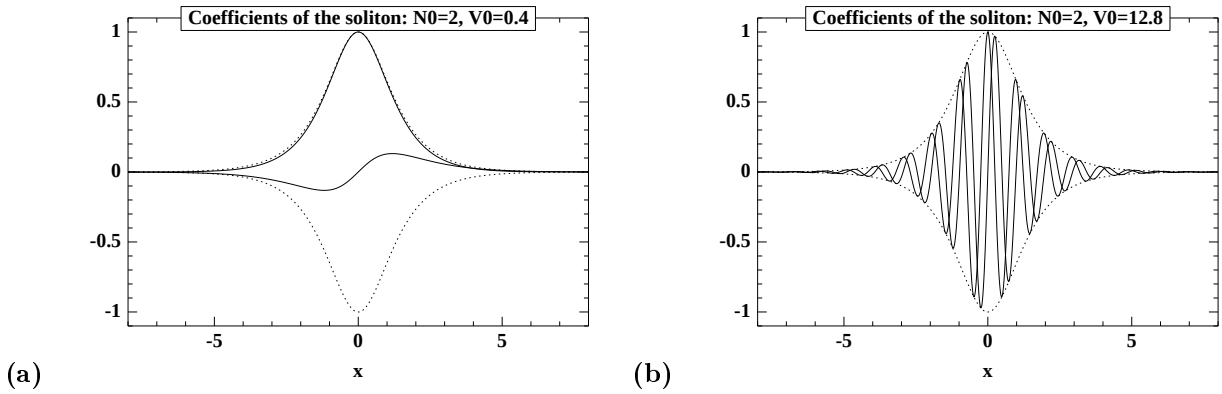

Figure 1. Solitons at time $t = 0$. The dashed lines represent the envelops of the solitons, while the solid lines represent the real and imaginary parts.

4. CONSERVED QUANTITIES AND SOLITON

There exists an infinite number of quantities which are preserved by the homogeneous NLS equation.[19] They can be represented as functionals of the solution u or in terms of the scattering data. We shall present here only two of them which are of physical interest.

• The mass of the wave $N = \int |u|^2 dx$. Denoting $n(\lambda) = -\pi^{-1} \ln |a(\lambda)|^2$, the mass is also given by

$$N = \sum_r 2i(\lambda_r^* - \lambda_r) + \int n(\lambda) d\lambda. \tag{10}$$

• The Hamiltonian or energy $H = \int |u_x|^2 - |u|^4 dx$, which can also be expressed as

$$H = \sum_r \frac{8i}{3}(\lambda_r^{*3} - \lambda_r{}^3) + 4 \int \lambda^2 n(\lambda) d\lambda. \tag{11}$$

There exists a special solution with finite mass and energy of Eq. (2) that is called soliton:

$$u_0(t,x) = 2\nu_0 \frac{\exp i\left(2\mu_0(x - 4\mu_0 t) + 4(\nu_0^2 + \mu_0^2)t\right)}{\cosh\left(2\nu_0(x - 4\mu_0 t)\right)}. \tag{12}$$

The mass and the velocity of the soliton are respectively $N_0 = 4\nu_0$ and $V_0 = 4\mu_0$. The width of the envelop of the soliton is conversely proportional to its mass. The soliton (12) is associated with the following scattering data:

$$a_0(\lambda) = \frac{\lambda - (\mu_0 + i\nu_0)}{\lambda - (\mu_0 - i\nu_0)}, \quad b_0(\lambda) = 0. \tag{13}$$

a_0 admits a unique zero in the upper complex half-plane denoted by $\lambda_0 = \mu_0 + i\nu_0$. The coefficient associated with the zero λ_0 is $\rho_0 = i \exp\left(-4i(\mu_0 + i\nu_0)^2 t\right)$. Fig. 1 plots two different solitons at time $t = 0$. Both have the same mass, and consequently the same envelop, but they have different velocities. Note that, in the case $\nu_0 \gg \mu_0$ (resp. $\nu_0 \ll \mu_0$), the soliton oscillates slowly (resp. quickly) within its envelop.

5. SOLITONS IN RANDOM MEDIA

We consider a perturbed Schrödinger equation with a non-zero right-hand side:

$$iu_t + u_{xx} + 2|u|^2 u = \varepsilon R(u)(t,x). \tag{14}$$

The small parameter $\varepsilon \in (0,1)$ characterizes the amplitude of the perturbation. The model of the perturbation is taken to be:

$$R(u)(t,x) = m_1(x)u(t,x) + m_2(x)|u|^2u(t,x) + (m_3(x)u_x)_x\,.$$

We shall assume that the incoming wave is a soliton incoming from the left and that m_1, m_2, and m_3 are random, stationary, ergodic, zero-mean, and independent processes. We aim at showing that, for a slab of size L/ε^2, the two following statements hold true in the limit $\varepsilon \to 0$. First the transmitted wave consists of a soliton plus some scattered waves. Second the soliton dynamics for almost every realization is described by non random evolution equations, where only the Fourier transforms of the autocorrelation functions of the random processes appear. From the physical point of view this fact was earlier established by Doucot and Rammal.[20] The remainder of the paper is devoted to the rigorous statements and discussions of these assertions.

First note that it is necessary to assume that the processes m_j fulfill some technical conditions, namely that there exists a function $z \mapsto \phi(z)$ vanishing as $z \to +\infty$ such that:[21]

$$\sup_{s>0}\left\{\mathbb{P}(B/A) - \mathbb{P}(B), A \in \mathcal{F}_0^s, B \in \mathcal{F}_{s+z}^\infty\right\} \leq \phi(z),$$

where $\mathcal{F}_s^z$ is the natural filtration associated to the processes m_j:

$$\mathcal{F}_s^z = \sigma(m_j(x), s \leq x \leq z, j = 1,2,3).$$

Roughly speaking $\phi(z)$ is proportional to the coherence degree of the process m_j evaluated at two points distant from z. The following results have been demonstrated in the case when the function $z \mapsto \phi(z)$ decays at least as z^{-4}. However we believe that this hypothesis can be weakened and we expect the condition $\int_0^\infty \phi^{1/2}(z)dz < \infty$ to be sufficient. The proof of the following proposition is sketched out in the appendix.

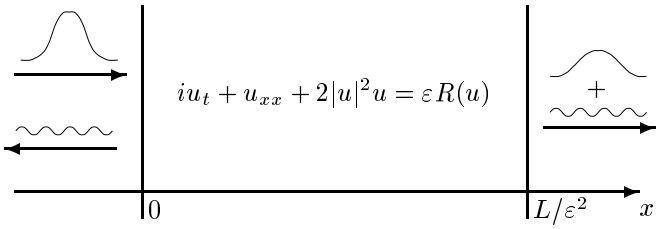

Figure 2. Scattering of a soliton.

Proposition 1. *Let us consider a slab of size L/ε^2.*
1. With probability that goes to 1 as $\varepsilon \to 0$, the scattered wave consists of one transmitted soliton plus some radiation.
2. The coefficients of the transmitted soliton converge in probability to the deterministic functions $\nu_l(L)$, $\mu_l(L)$ which satisfy the system of ordinary differential equations:

$$\left\{\begin{array}{l} \dfrac{d\nu_l}{dx} = F(\nu_l,\mu_l), \quad \nu_l(0) = \nu_0, \\ \dfrac{d\mu_l}{dx} = G(\nu_l,\mu_l), \quad \mu_l(0) = \mu_0, \end{array}\right. \tag{15}$$

where F and G are deterministic functions where only the Fourier transforms of the autocorrelation functions appear:

$$\begin{aligned} F(\nu,\mu) &= -\frac{1}{2\pi}\sum_{j=1}^{3}\int_{-\infty}^{\infty}|c_j|^2(\nu,\mu,\lambda)\alpha_j(k(\nu,\mu,\lambda))d\lambda, \\ G(\nu,\mu) &= -\frac{1}{4\pi}\sum_{j=1}^{3}\int_{-\infty}^{\infty}\left(\frac{\lambda^2}{\mu\nu} + \frac{\nu}{\mu} - \frac{\mu}{\nu}\right)|c_j|^2(\nu,\mu,\lambda)\alpha_j(k(\nu,\mu,\lambda))d\lambda. \end{aligned}$$

The coefficients α_j and k are defined by:

$$\alpha_j(k) = \int_0^\infty \mathbb{E}[m_j(0)m_j(x)]\cos(kx)dx, \qquad k(\nu,\mu,\lambda) = \frac{(\lambda-\mu)^2+\nu^2}{\mu}.$$

The functions c_j can be computed explicitly:

$$\begin{aligned}
c_1(\nu,\mu,\lambda) &= \frac{\pi}{2^4\mu^3}\frac{(\lambda-\mu+i\nu)^2}{\cosh\left(\pi(\mu^2-\nu^2-\lambda^2)/(4\mu\nu)\right)},\\
c_2(\nu,\mu,\lambda) &= \frac{\left((\lambda+\mu)^2+\nu^2\right)\left(\nu^2+17\mu^2-6\lambda\mu+\lambda^2\right)}{12\mu^2}c_1(\nu,\mu,\lambda),\\
\tilde{c}(\nu,\mu,\lambda) &= \frac{\left((\lambda-\mu)^2+\nu^2\right)^2+8\mu^2(-\nu^2+\mu\lambda-\mu^2)}{3\mu\left((\lambda-\mu)^2+\nu^2\right)}c_1(\nu,\mu,\lambda),\\
c_3(\nu,\mu,\lambda) &= (4(\nu^2-\mu^2)c_1-4\mu\tilde{c}-2c_2)+i(2\mu c_1+\tilde{c})k(\nu,\mu,\lambda).
\end{aligned}$$

Note that $\alpha_j(k)$ is nonnegative since it is proportional to the k-frequency evaluation of the power spectral density of the stationary process m_j by Wiener-Khintchine theorem.[22] The analysis of the effective system (15) exhibits several possible regimes. Two of them are stable and attractive, the first one being characterized by a logarithmic decay of the velocity for solitons of sufficiently large mass, and the second one by an exponential decay of the mass for solitons of small mass. There are also intermediate regimes where both the mass and the velocity decrease at a polynomial rate. More exactly:

1) If the mass of the incoming soliton is small (below a critical value depending on $\alpha_j(.)$ and μ_0), then the velocity of the soliton is almost constant, while its mass decreases to 0 as a function of the size of the slab L:
- as $\exp(-L/L_{loc})$, where $L_{loc}=32\mu_0^2/\alpha_1(4\mu_0)$ (perturbation of the linear potential),[23]
- as $L^{-1/4}$ (perturbation of the nonlinear coefficient),[23]
- as $L^{-1/2}$, then as $\exp(-L/L'_{loc})$ (dispersive perturbation).[24]

2) If the mass of the soliton is large enough, then the mass of the soliton is almost constant, while its velocity of the soliton slowly decreases to 0. The decay rate depends on the tail of the spectrum of the perturbation, but we can state in great generality that it is at most logarithmic. For instance, if $\mathbb{E}[m_1(0)m_1(x)]=\sigma^2(1-|x|/l_c)\mathbf{1}_{|x|\le l_c}$, then

$$\lim_{L\to\infty}\mu_l(L)\times\ln(L)=\frac{\pi\nu_0}{2},$$

which means that the velocity decreases as the logarithm of the length. However the decay rate may be much slower. As an example, if the autocorrelation function is $\mathbb{E}[m_1(0)m_1(x)]=\sigma^2\exp(-x^2/l_c^2)$, then the velocity decreases as the square root of the logarithm of L:

$$\lim_{L\to\infty}\mu_l(L)\times\sqrt{\ln(L)}=\frac{\nu_0^2 l_c}{2}.$$

It can be noted that, in the limit case $\nu_0/\mu_0\to 0$, the incoming soliton can be approximated by a linear wavepacket:

$$u_0(t,x)\simeq\int_{-\infty}^{+\infty}dk f(k)e^{ikx-ik^2t},\ \text{with } f(k)=\frac{1}{2}\cosh^{-1}\left(\frac{\pi}{4}\left(\frac{k-2\mu_0}{\nu_0}\right)\right),$$

whose spectrum is narrow around the carrier wavenumber $k_0=2\mu_0$. The result is in agreement with the linear approximation, since the localization length L_{loc} corresponding to a perturbation of the linear potential can be written in terms of the carrier wavenumber as $L_{loc}=8k_0^2/\alpha_1(2k_0)$. It is equal to the localization length of a monochromatic wave with wavenumber k_0 scattered by a slab of random linear medium.[25]

6. NUMERICAL SIMULATIONS

The results in the previous sections are theoretically valid in the limit case $\varepsilon\to 0$, where the amplitudes of the perturbations go to zero and the size of the random slab goes to infinity. In this section we aim at showing that the asymptotic behaviors of the soliton can be observed in numerical simulations in the case where ε is small, more precisely smaller than any other characteristic scale of the problem. We use a fourth-order split-step method to simulate the perturbed nonlinear Schrödinger equation (14). This numerical algorithm provides accurate and stable solutions.[16] For the sake of simplicity we only consider perturbations of the linear potential m_1 and take $m_2=m_3=0$.

Let Δt be the elementary time step and h be the elementary space step. Let us denote by $\left(u^0(jh)\right)_{j=-K,\dots,K-1}$ the initial wave solution. By induction we compute u^{n+1} from $u^n := (u(n\Delta t, jh))_{j=-K,\dots,K-1}$:

$$\begin{aligned} \text{first step:} \quad & u^{n+1/3} = A(\Delta t/2)u^n, \\ \text{second step:} \quad & u^{n+2/3} = B(\Delta t)u^{n+1/3}, \\ \text{third step:} \quad & u^{n+1} = A(\Delta t/2)u^{n+2/3}, \end{aligned}$$

where $A(\Delta t/2)$ is the linear operator generated by $i\partial_x^2$ and B is simply a scalar multiplication in the physical space by $\exp i\left(2|u|^2 - \varepsilon m_1\right)\Delta t$. The first and third steps can be solved using a Fourier transform. Indeed, in Fourier space the effect of the exponential operator $A(\Delta t/2)$ is a scalar multiplication by $\exp -i(k^2\Delta t/2)$.

To sum up, the split step algorithm involves a sequence of steps that include free-space propagation over a half-step, then a nonlinear correction, and free space propagation over the final half-step. Practically, it is easy to see that the two back-to-back free-space half-steps can be combined into a single free-space step over Δt. The error of the split-step algorithm comes from the splitting process, because the operators A and B do not commute. It is well-known that the method described here above is of second-order.[11] However, since the NLS equation is time reversible, we can use a standard method which transforms a second-order method into a fourth-order method.[26] Indeed, if $C(\Delta t)u(t,x)$ is a second-order approximation to $u(t+\Delta t, x)$, then $C(\alpha\Delta t)C(-\beta\Delta t)C(\alpha\Delta t)u(t,x)$ is a fourth-order approximation to $u(t+\Delta t, x)$, if we take care to choose $\alpha = 1/(2-2^{1/3})$ and $\beta = 2^{1/3}/(2-2^{1/3})$. The drawback of this method is that we implicitly impose periodicity on the solutions because of the Fourier transform that is used on a finite interval. We can control it by using a shifting computational domain which is always centered at the center of the mass of the solution. Moreover we shall impose boundaries of this domain which absorb outgoing waves. This can be readily achieved by adding a complex potential which is smooth so as to reduce reflections. We choose to substitute the complex potential $m(x) = m_1(x) - i m_{abs}(x)$ for the random potential $m_1(x)$:

$$m_{abs}(x) = \begin{cases} m_{abs\,max} \sin^2\left(\dfrac{\pi}{2}\dfrac{x_l - x}{x_l - X_l}\right) & \text{, if } X_l \le x < x_l, \\ 0 & \text{, if } x_l \le x < x_r, \\ m_{abs\,max} \sin^2\left(\dfrac{\pi}{2}\dfrac{x - x_r}{X_r - x_r}\right) & \text{, if } x_r \le x < X_r, \end{cases}$$

where X_l (resp. X_r) is the left (resp. right) end of the computational domain, and $[X_l, x_l]$ (resp. $[x_r, X_r]$) is the left (resp. right) absorbing slab. The energy (or Hamiltonian) defined by (18) is theoretically preserved by the split-step method up to the machine accuracy in case of a truly periodic situation without absorption. The domain that we consider is not periodic, since it shifts along the simulation and the outgoing wave is absorbed by an imaginary potential at the boundaries of the domain. However the size of the shifting domain is taken so that the distortion imposed by the non-periodicity has a negligible effect.

We assume in this section that the potential is constant over elementary intervals of length l_c and take independent random values over each interval:

$$m_1(x) = A_i \text{ if } il_c \le x < (i+1)l_c, \quad i = 0, \dots, M,$$

where $(A_i)_{i\in\mathbb{N}}$ is a sequence of independent and identically distributed variables which obey uniform distributions over the interval $[-1,1]$. The autocorrelation function of the ergodic process m_1 is equal to $\frac{1}{3}(1 - |x|/l_c)\mathbf{1}_{|x|\le l_c}$. The integer M which is proportional to the size of the random slab will be chosen so large that we can observe the effect of the small perturbation εm_1. We measure the mass (i.e. the L^2-norm) and center of the solution during the propagation, and also the envelop of the transmitted solution, that we can compare with the envelop of the incoming soliton. The mass $N(n\Delta t)$ and the center $C(n\Delta t)$ are computed at time $n\Delta t$ from the data $(u(n\Delta t, jh))_{j=-K,\dots,K-1}$ as:

$$N(n\Delta t) = h \times \sum_{j=-K}^{K-1} |u(n\Delta t, jh)|^2, \quad C(n\Delta t) = h \times \sum_{j=-K}^{K-1} |u(n\Delta t, jh)|^2 j / N(n\Delta t).$$

We finally deal with the set of data $(C(n\Delta t))_n$ in order to compute the velocity of the solution, defined here as the time-derivative of the center. We present simulations where the initial wave at time $t = 0$ is a soliton with mass $N_0 = 2$ and velocity $V_0 = 1.6$ centered at $x = 0$ (see Fig. 3a). In the first one we simulate the homogeneous

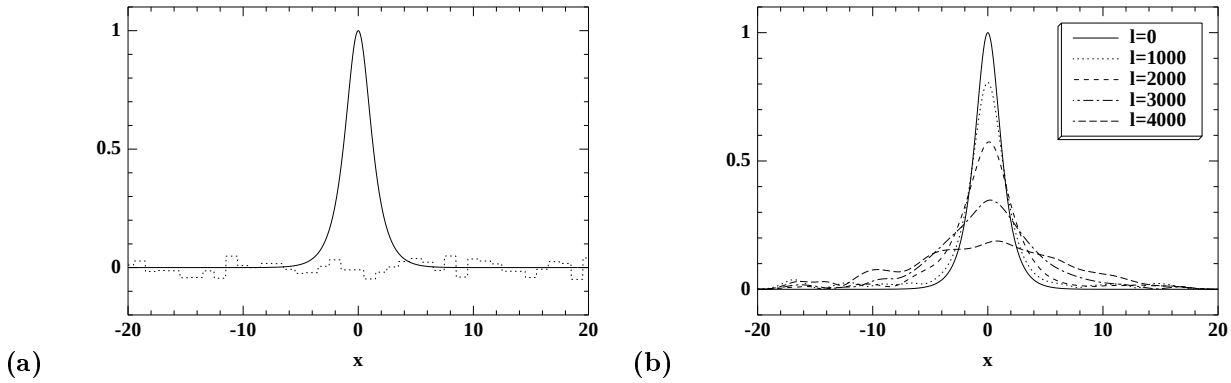

Figure 3. Picture (a): Envelop of the initial soliton (solid line) whose mass is $N_0 = 2$ and velocity $V_0 = 1.6$. In dashed line is plotted the profile of one realization of the random potential εm_1 with $\varepsilon = 0.05$ and $l_c = 0.4$. Picture (b): Envelops of the soliton when its center crosses different depth lines l for one of the realization of the random potential. The coordinate x is normalized around the depth line l.

nonlinear Schrödinger equation (2), which admits as an exact solution (12). We can therefore check the accuracy of the numerical method, since we can see that the computed solution maintains a very close resemblance to the initial soliton (data not shown), while the mass and velocity are almost constant. The seven other simulations are carried out with seven different realizations of the random potential with $\varepsilon = 0.05$ and $l_c = 0.4$. The simulated evolutions of the coefficients of the soliton are presented in Fig. 4 and compared with the theoretical evolutions given by (15) in the scale x/ε^2. It thus appears that the numerical simulations are in very good agreement with the theoretical results. The simulated masses follow very closely the theoretical ones. This is partly due to the fact that the split-step method preserves the total mass:

$$N_{tot} = 4\nu + \int_{-\infty}^{\infty} n(\lambda) d\lambda, \tag{16}$$

where $n(\lambda)$ is the density of scattered mass at frequency 2λ. This implies stability for the coefficient ν and the mass of the soliton. The results may seem a bit less convincing when one looks at the velocity. Indeed the split-step method preserves the total energy which can be expressed from (11) and (18) as:

$$E_{tot} = 16\left(\nu\mu^2 - \frac{\nu^3}{3}\right) + 4\int_{-\infty}^{\infty} \lambda^2 n(\lambda) d\lambda + \varepsilon \int m_1(x)|u|^2 + \frac{1}{2} m_2(x)|u|^4 - m_3(x)|u_x|^2 dx. \tag{17}$$

The last term is negligible in the asymptotic framework $\varepsilon \to 0$, but when $\varepsilon = 0.05$ it gives rise to local fluctuations of the coefficient μ and of the instantaneous velocity of the soliton. The velocities plotted in Fig. 4 have actually been smoothed by averaging over intervals of length $\Delta x_{ave} = 20$. This instability could explain the slight dispersal of the lines plotting the simulated velocities. Fig. 3b plots the envelops of the solution at different depths corresponding to one of the simulations, which shows that the wave keeps the basic form of a soliton although it looses some mass. All these results confirm that system (15) describes with accuracy the transmission of a soliton through a random slab for small perturbations and large slabs.

7. CONCLUSION

We have studied the propagation of a soliton in a nonlinear dispersive medium with spatially random perturbations by applying the powerful inverse scattering transform. If the incoming soliton has large mass, we have shown that the mass of the soliton is almost constant. Furthermore the velocity is found to decrease at a slow rate (at most logarithmic) which depends on the high-frequency behavior of the power spectrum of the spatial dispersive random perturbation. In case of small mass, we have proved that the mass of the soliton decays to zero exponentially or algebraically with the length of the system.

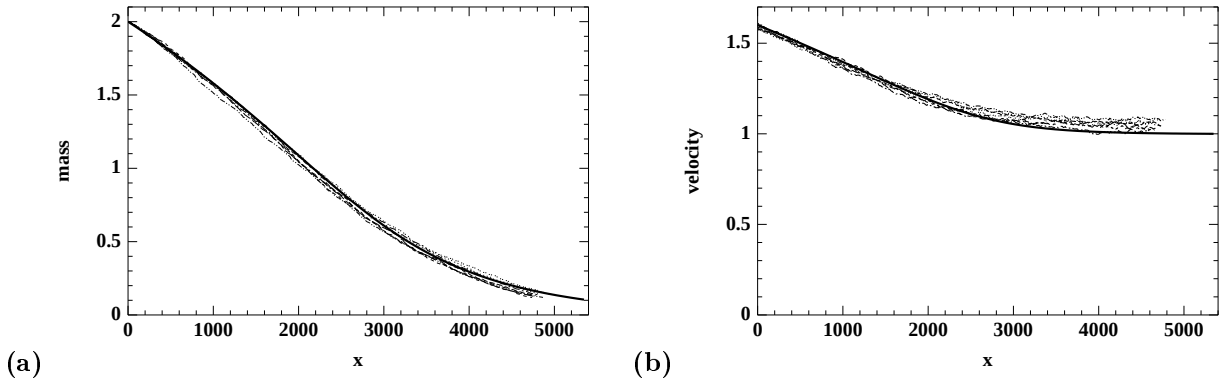

Figure 4. Coefficients of the transmitted soliton whose initial coefficients are $N_0 = 2$, $V_0 = 1.6$ with a random potential whose amplitude is $\varepsilon = 0.05$ and correlation length $l_c = 0.4$. Picture (a) (resp. picture (b)) is devoted to the mass (resp. velocity). The thick solid lines represent the theoretical coefficients of the transmitted soliton. In thin dotted lines are plotted the simulated coefficients of the soliton when no random potential is present. In thin dashed and dotted lines are plotted the simulated masses and velocities of the transmitted solitons for 7 different realizations of the random potential.

We feel that it should be of great interest to consider other integrable systems with a different type of dispersion. For instance the Korteweg-de Vries equation, with a third order dispersion, is worth studying. Besides the interaction of solitons in random dispersive media represents also a challenge for practical applications to telecommunications.

APPENDIX A. PROOF OF PROPOSITION 1

We now list the main steps of the proof.[23,24]

a. A priori estimates.
The following quantities (mass and energy) are preserved by the perturbed Schrödinger equation (14):

$$N_{tot} = \int |u|^2 dx, \quad E_{tot} = \int |u_x|^2 - |u|^4 dx + \varepsilon \int H_1(x) dx, \qquad H_1(x) := m_1(x)|u|^2 + \frac{1}{2} m_2(x)|u|^4 - m_3(x)|u_x|^2. \quad (18)$$

Assume that the m_j are bounded processes. Sobolev inequalities then prove that the H^1-norm, the L^4-norm and the L^∞-norm of $u(t,.)$ are uniformly bounded with respect to $t \in \mathbb{R}$ and $\varepsilon \in (0,1)$. Furthermore $\varepsilon \int H_1(x) dx$ can be bounded uniformly with respect to $t \in \mathbb{R}$ by $K(N_{tot}, E_{tot})\varepsilon$.

b. Prove the stability of the zero of the Jost coefficient a.
The zero corresponds to the soliton. This part strongly relies on the analytical properties of a in the upper complex half plane. Basically we apply Rouché's theorem so as to prove that the number of zeros is constant. This method is efficient to prove that the zero is preserved, but it does not bring control on its precise location in the upper half plane. This step is not sufficient to compute the variations of the soliton parameters.

c. Compute the radiation.
The Jost coefficients a and b satisfy coupled equations[27]:

$$\begin{cases} \dfrac{\partial a(\lambda,t)}{\partial t} &= 0 &+\varepsilon \left(a(\lambda,t)\bar{\gamma}(\lambda,t) + b(\lambda,t)\gamma(\lambda,t)\right), \\ \dfrac{\partial b(\lambda,t)}{\partial t} &= -4i\lambda^2 b(\lambda,t) &-\varepsilon \left(a(\lambda,t)\gamma^*(\lambda,t) + b(\lambda,t)\bar{\gamma}(\lambda,t)\right), \end{cases}$$

where $\gamma(\lambda,t) = -\int dx R(u) f_2^2 + R(u)^* f_1^2$ and $\bar{\gamma}(\lambda,t) = -\int dx R(u)^* f_1^* f_2 - R(u) f_1 f_2^*$. From these equations we can estimate the amount of radiation which is emitted during some time interval in terms of mass and energy thanks

to (10) and (11). We are then able to deduce the evolution equations of the coefficients of the soliton by using the conservations of the total mass and energy. For times of order $O(1)$, since N_{tot} and E_{tot} are conserved, the variations $\Delta(..)$ of the relevant quantities are linked together by the relations:

$$\begin{aligned} 0 &= 4\Delta\nu + \int \Delta n(\lambda) d\lambda, \\ 0 &= 16\Delta\left(\nu\mu^2 - \nu^3/3\right) + 4\int \lambda^2 \Delta n(\lambda) d\lambda + \varepsilon\Delta\left(\int_{\mathbb{R}} H_1(x)dx\right). \end{aligned}$$

$\Delta n(\lambda)$ is of order ε^2, but the last term in the expression of the total energy is of order ε. Thus our strategy is not efficient for estimating the variations of the coefficients of the soliton for times of order $O(1)$. Let us now consider times of order $O(\varepsilon^{-2})$. $\Delta n(\lambda)$ is now of order 1, while the last term in the expression of the total energy is of order ε by the a priori estimates. Thus we can efficiently compute the long-time behavior of the coefficients of the soliton in the asymptotic framework $\varepsilon \to 0$, when the last term in the expression of the total energy is uniformly negligible. Applying probabilistic limit theorems (approximation-diffusion), we then find that the coefficients of the soliton converge in probability to non-random functions which satisfy the system (15).

d. Compute the form of the scattered wave.
Neglecting the terms of higher order, the total wave is given by the sum $u(t/\varepsilon^2, x) = u_S(t/\varepsilon^2, x) + u_L(t/\varepsilon^2, x)$, where u_S is a soliton of mass $4\nu(t/\varepsilon^2)$ and velocity $4\mu(t/\varepsilon^2)$:

$$u_S(\frac{t}{\varepsilon^2}, x) = -2i\nu \frac{\exp i\left(2\mu(x - x_s) + \phi_s\right)}{\cosh\left(2\nu(x - x_s)\right)}, \tag{19}$$

x_s and ϕ_s are respectively the position and the phase of the soliton at time t/ε^2:

$$x_s = \frac{1}{2\nu}\ln\left(\frac{1}{2\nu}\left|\frac{\rho_r(t/\varepsilon^2)}{a'(t/\varepsilon^2, \lambda_s)}\right|\right), \quad \phi_s = \arg\left(-i\frac{\rho_r(t/\varepsilon^2)}{a'(t/\varepsilon^2, \lambda_s)}\right) + 2\mu x_s, \tag{20}$$

$\lambda_s = \mu(t/\varepsilon^2) + i\nu(t/\varepsilon^2)$ and u_L admits the following expression:

$$\begin{aligned} u_L(\frac{t}{\varepsilon^2}, x) = \; & \frac{1}{i\pi}\int_{-\infty}^{\infty} \frac{b}{a}(\lambda) \frac{\left(\lambda - \mu + i\nu\tanh\left(2\nu(x - x_s)\right)\right)^2}{(\lambda - \mu + i\nu)^2} e^{2i\lambda x} d\lambda \\ & + \frac{\nu^2}{i\pi} \frac{\exp 2i\left(2\mu(x - x_s) + \phi_s\right)}{\cosh^2\left(2\nu(x - x_s)\right)} \int_{-\infty}^{\infty} \frac{b^*}{a^*}(\lambda) \frac{1}{(\lambda - \mu - i\nu)^2} e^{-2i\lambda x} d\lambda. \end{aligned} \tag{21}$$

u_S is the soliton part of the total wave. The first component of u_L represents the radiated wavepacket, with a correction in the neighborhood of the soliton $x \sim x_s(t/\varepsilon^2)$. The second component of u_L represents the interaction of the soliton and the radiation, which is only noticeable in the neighborhood of the soliton. This result is not surprising. Roughly speaking, the support of the radiation lies in an interval with length of order ε^{-2}. Since the L^2-norm is bounded by the conservation of the total mass, we can expect that the amplitude of the radiation is of order ε. More exactly it can be rigorously proved that the amplitude of the radiated wavepacket can be bounded above by $K\varepsilon|\ln\varepsilon|$.[23]

REFERENCES

1. I. M. Lifshitz, S. A. Gredeskul, and L. Pastur, *Introduction to the theory of disordered systems*, Wiley, New York, 1988.
2. R. Knapp, G. Papanicolaou, and B. White, "Transmission of waves by a nonlinear random medium," *J. Stat. Phys.* **63**, pp. 567-583, 1991.
3. P. Devillard and B. Souillard, "Polynomially decaying transmission for the nonlinear Schrödinger equation in a random medium," *J. Stat. Phys.* **43**, pp. 423-439 ,1986.
4. B. Doucot and R. Rammal, "On Anderson localization in nonlinear random media," *Euro. Phys. Lett.* **3**, pp. 969-974, 1987.

5. Y. U. Kivshar, A. M. Kosevich, and O. A. Chubykalo, "Resonant and non resonant soliton scattering by impurities," *Phys. Lett. A* **125**, pp. 35-40, 1987.
6. D. J. Korteweg and G. de Vries, "On the change of form of long waves advancing in a rectangular canal, and on a new type of long stationary waves," *Philos. Mag. Ser.* **39**, pp. 422-443, 1895.
7. J. Boussinesq, "Théorie de l'intumescence liquide appelée onde solitaire ou de translation, se propageant dans un canal rectangulaire," *C. R. Acad. Sci. Paris* **72**, pp. 755-759, 1871.
8. C. S. Gardner, J. M. Greene, M. D. Kruskal, and R. M. Miura, "Method for solving the Korteweg-de Vries equation," *Phys. Rev. Lett.* **19**, pp. 1095-1097, 1967.
9. P. D. Lax, "Integrals of nonlinear equations of evolution and solitary waves," *Comm. Pure Appl. Math.* **21**, pp. 467-490, 1968.
10. V. E. Zakharov and A. B. Shabat, "Exact theory of two-dimensional self-focusing and one-dimensional self-modulation of waves in nonlinear media," *Sov. Phys. JETP* **34**, pp. 62-69, 1972.
11. A. C. Newell and J. V. Moloney, *Nonlinear optics*, Addison-Wesley, Redwood City, 1992.
12. A. Hasegawa and F. Tappert, "Transmission of stationary nonlinear optical pulses in dispersive dielectric fibers, I; Anomalous dispersion," *Appl. Phys. Lett.* **23**, pp. 142-144, 1973.
13. Y. U. Kivshar, S. A. Gredeskul, A. Sanchez, and L. Vasquez, "Localization decay induced by strong nonlinearity in disordered systems," *Phys. Rev. Lett.* **64**, pp. 1693-1696, 1990.
14. *Nonlinearity with Disorder*, F. Kh. Abdullaev, A. R. Bishop, and St. Pnevmatikos, eds., Springer, Berlin ,1991.
15. S. A. Gredeskul and Y. U. Kivshar, "Propagation and scattering of nonlinear waves in disordered systems," *Phys. Rep.* **216**, pp. 1-61, 1992.
16. R. Knapp, "Transmission of solitons through random media," *Physica D* **85**, pp. 496-508, 1995.
17. J. C. Bronski, "Nonlinear wave propagation in a disordered medium," *J. Stat. Phys.* **92**, pp. 995-1015, 1998.
18. M. J. Ablowitz and H. Segur, *Solitons and the inverse scattering transform*, SIAM, Philadelphia, 1981.
19. S. V. Manakov, S. Novikov, J. P. Pitaevskii, and V. E. Zakharov, *Theory of solitons*, Consultants Bureau, New York, 1984.
20. B. Doucot and R. Rammal, "Invariant imbedding approach to localization," *J. Physique* **48**, pp. 527-546, 1987.
21. H. J. Kushner, *Approximation and weak convergence methods for random processes*, MIT Press, Cambridge, 1984.
22. D. Middleton, *Introduction to statistical communication theory*, Mc Graw Hill Book Co., New York, 1960.
23. J. Garnier, "Asymptotic transmission of solitons through random media," *SIAM J. Appl. Math.* **58**, pp. 1969-1995, 1998.
24. F. Kh. Abdullaev and J. Garnier, "Solitons in media with random dispersive perturbations," *Physica D* **134**, pp. 303-315, 1999.
25. L. Arnold, G. Papanicolaou, and V. Wihstutz, "Asymptotic analysis of the Lyapunov exponent and rotation number of the random oscillator and applications," *SIAM J. Appl. Math.* **46**, pp. 427-450, 1986.
26. H. Yoshida, "Construction of higher order symplectic integrators", *Phys. Lett. A* **150**, pp. 262-268, 1990.
27. V. I. Karpman, "Soliton evolution in the presence of perturbations," *Phys. Scr.* **20**, pp. 462-478, 1979.